Hindawi Publishing Corporation
Journal of Nanomaterials
Volume 2012, Article ID 753429, 9 pages
doi:10.1155/2012/753429

*Research Article*

# Efficient Visible Light Photocatalytic Oxidation of NO on F- and N-Codoped Spherical $TiO_2$ Synthesized via Ultrasonic Spray Pyrolysis

**Jianhui Huang,[1,2] Wahkit Cheuk,[2] Yifan Wu,[3] Frank S. C. Lee,[3] and Wingkei Ho[4]**

[1] *Environmental and Life Sciences Department, Putian University, Putian 351100, China*
[2] *Nano and Advanced Materials Institute Limited, The Hong Kong University of Science and Technology, Hong Kong*
[3] *Department of Civil and Structural Engineering, Research Center for Environmental Technology and Management, The Hong Kong Polytechnic University, Hong Kong*
[4] *Department of Science and Environmental Studies, The Hong Kong Institute of Education, Hong Kong*

Correspondence should be addressed to Jianhui Huang, owenhuang95@163.com and Wingkei Ho, keithho@ied.edu.hk

Received 8 June 2012; Accepted 3 October 2012

Academic Editor: Gong Ru Lin



The fluorine- and nitrogen-codoped $TiO_2$ was synthesized by ultrasonic spray pyrolysis method with titanium tetrafluoride and urea as precursor. The codoped $TiO_2$ was characterized by X-ray diffractometry (XRD), scanning electron microscopy (SEM), transmission electron microscopy (TEM), diffuse reflectance spectroscopy (DRS), and X-ray photoelectron spectroscopy (XPS). Nitric oxide (NO) photocatalytic oxidation in gas-phase medium was employed as a probe reaction to evaluate the photocatalytic reactivity of the catalysts. The results indicated that spherical codoped $TiO_2$ photocatalysts with unique puckered surface were obtained by this method. The codoped catalysts have solely anatase crystalline structure. The optical characterization of the codoped catalysts showed that the codoped samples could be excited by visible light photons in the 400–550 nm and could efficiently oxidize NO under visible light irradiation. The mechanism of special morphology formation of prepared codoped $TiO_2$ structure is also discussed.

## 1. Introduction

Growing knowledge about the indoor air quality (IAQ) has validated it as one of the major risks of the human health as people spend more than 80% of their time indoors in most countries [1]. Thus, more and more attentions have been drawn into developing a green process of eliminating pollutants from indoor air. Several physical and chemical methods for treating the pollutant in the indoor air have been studied extensively, including adsorption [2, 3], ozonation [4], plasma [5], and photocatalytic oxidation [6–9]. Among these, semiconductor-mediated photocatalysis is one of the most efficient destructive technologies because of its high redox ability, nonselectivity, at-room temperature, and atmospheric pressure. For decades, titanium dioxide ($TiO_2$) has been accepted as one of the most promising photocatalysts owning to its intrinsic properties such as inexpensiveness, high chemical stability, and low toxicity. Unfortunately, a major obstacle in the popularization of $TiO_2$ is its large band gap (3.2 eV) which work only under specific UV light region ($\lambda < 380$ nm), hence, practically ruling out most of the solar energy for the environmental remediation. Thus, considerable efforts have been devoted to modified $TiO_2$ in order to broaden the light response range of $TiO_2$-base photocatalysts which is still a significant issue in both academic and practical applications. Doping $TiO_2$ with various elements has been proved as an effective method to optimize the band structure of $TiO_2$, and thereby in resulting to be a visible-light sensitive photocatalyst. While the cations doping $TiO_2$ are often impaired by thermal instability and an increase in the population of recombination centers, thus no significant results were achieved [10, 11]. Doping $TiO_2$ with nonmetal such as N, C, S, B, and P seems to be more efficient to address this problem in certain extend [12–18]. Among them, doping with nitrogen atom is considered

to be one of the most effective way to obtain visible-light-driven photocatalytic activity [19, 20]. However, the reactivity or quantum efficiency is still not high enough with only doping nitrogen. Thus many researches were designed to be codoped with other nonmetal element such as C, S, B, and P [21–24] via the synergistic effects between two dopants to further enhance the photocatalytic efficiency. Among them, intense interest has been shown on the F- and N-codoped $TiO_2$ [25–30]. The doping of fluorine will have effect on the physicochemical properties of $TiO_2$ in many aspects [31]. The study of Yu et al. indicated that the fluorine doping would result in the formation of reduced $Ti^{3+}$ ions and surface oxygen vacancies which may promote charge separation and improve the efficiency of photoinduced processes [32]. Vijayabalan reported that the fluorination enhanced the absorbance of $TiO_2$ in the UV-visible region which is favorable to the visible-light photocatalytic activity of $TiO_2$ [33]. The doping of fluorine was also found to have side effect, for example, it would lower the conduction band which leads to a lower photocatalytic activity in some photocatalytic reactions [34]. Thus it is meaningful to further study the properties of N- and F-codoped $TiO_2$ and the synergistic effects between the N and F dopants in the catalyst.

Synthetic methods such as sol-gel and hydrothermal technique have been widely used to make codoped $TiO_2$ photocatalyst which have advantages including precise control of pore structure, dopant concentration, and chemical purity [35–37]; however, they require severe conditions such as long time for reaction or high-pressure resistant equipment which is not easy to produce in large scale. Thus, a high-yield synthetic method that is capable of producing nanostructure $TiO_2$ with controllable dopant concentration and crystallinity will undoubtedly benefit the design of high-performance materials in the catalyst industry. Ultrasonic spray pyrolysis is a convenient method for the facile mass production of nanostructured spherical materials because of its simple and inexpensive apparatus and easy control of product composition. Recently, carbon, $SiO_2$, $Bi_2WO_6$, $InVO_4$, and so forth have been synthesized by this method [38–41]. Although ultrasonic spray pyrolysis has been widely used to produce inorganic powders, it is still a challenge to fabricate in the prepared material decorated with heteroatom especially the nonmetal atoms.

In this study, we fabricated fluorine- and nitrogen-codoped $TiO_2$ using ultrasonic spray pyrolysis method with urea and titanium tetrafluoride as precursors. The as-prepared product had unique spherical structures with puckered surface and exhibited high photocatalytic activity on the oxidation of NO in air under the irradiation of visible light. The preparation method is simple and continuous which is easy for batch production. Moreover, the dopant of such $TiO_2$ sphere is easily controlled by regulating the experimental conditions.

## 2. Experimental Section

*2.1. Catalysts Preparation.* All of the chemicals were of commercially available analytical grade and used without further purification. Fluorine- and nitrogen-codoped $TiO_2$ photocatalysts were prepared by an ultrasonic spray pyrolysis method. In a typical process, $TiF_4$ (1.5 g) was added to 150 mL HCl solution (0.5 M) under magnetic stirring. After stirring for several minutes, a transparent colorless solution was obtained. Then, different quantity of urea (0, 1, 5, and 10 g) was added to the solution under magnetic stirring. After the urea was dissolved completely, the resulting solution was nebulized at 1.7 MHz ±10% (YUYUE402AI, Shanghai, China). The produced aerosol was carried with pumping air flow (5 L/min) through a quartz tube surrounded by a furnace thermostated. The pyrolysis proceeded quickly as aerosol passed through the high-temperature tube maintained at the temperature of 500°C. The quartz reaction tube with the diameter of 3.5 cm was 1 m long. The products were collected in a percolator with distilled water, then separated by centrifugation, washed thoroughly with ethanol and distilled water, and finally dried in an oven at 100°C for 1 h. A vivid yellow product was obtained. The as-prepared product was then further calcinated at 500°C and held for 1 h (ramp rate of 1°C/min). The samples prepared by addition of 1 g, 5 g, and, 10 g urea were designated FNT-1, FNT-5, and FNT-10, respectively. For comparison, the fluorine-doped $TiO_2$ was also prepared without adding urea and it was designated FT.

*2.2. Characterization.* The X-ray diffraction (XRD) patterns were recorded on a Bruker D8 Advance X-ray diffractometer with Cu Ka radiation ($\lambda = 1.54178$ A°) at a scan rate of 0.05° $2\theta$/s. The accelerating voltage and the applied current were 40 kV and 40 mA, respectively. Scanning electron microscopy (SEM, JSM-5600) was used to characterize the morphology of the obtained products. Transmission electron microscopy (TEM) study was carried out on a Philips CM-120 electron microscopy instrument. The samples for TEM were prepared by dispersing the final powders in methanol; the dispersion was then dropped on carbon copper grids. A Varian Cary 100 Scan UV-Visible system equipped with a labsphere diffuse reflectance accessory was used to obtain the reflectance spectra of the catalysts over a range of 200–800 nm. Labsphere USRS-99-010 was employed as a reflectance standard. The spectra were converted from reflection to absorbance by Kubelka-Munk method. X-ray photoelectron spectroscopy (XPS) measurements were performed on a PHI Quantum 2000 XPS system with a monochromatic Al K$\alpha$ source and a charge neutralizer. All the binding energies were calibrated to the C 1s peak at 284.8 eV of the surface adventitious carbon.

*2.3. NO Removal Test.* The nitric oxide (NO) is the common pollutant of indoor air. It was reported by WHO that it could lead to respiratory symptoms, bronchoconstriction, increased bronchial reactivity, airway inflammation, and decreases in immune defence leading to increased susceptibility to respiratory infection. Thus, we used NO photocatalytic oxidation to evaluate the performance of photocatalysts in this study. The NO removal with the resulting samples was performed at ambient temperature in

a continuous flow reactor. The volume of the rectangular reactor which was made of stainless steel and covered with Saint-Glass was 4.5 L (10 cm × 30 cm × 15 cm (H × L × W)). The sample to be tested was prepared by coating an aqueous suspension of the photocatalyst onto a dish with a diameter of 5.0 cm. The weight of the photocatalysts used for each experiment was kept at 0.3 g. The dishes containing the photocatalyst were pretreated at 70°C for several hours until a complete removal of water in the suspension and then cooled to room temperature before use. The lamp was vertically placed outside the reactor above the sample dish, and a glass filter was placed to cutoff light below 400 nm. Four minifans were fixed around the lamp to avoid the temperature rise of the flow system. Furthermore, adequate distance was also kept from the lamp to the reactor for the same purpose to avoid temperature rise. The NO gas was acquired from compressed gas cylinder at a concentration of 48 ppm NO ($N_2$ balance, BOC gas) with traceable National Institute of Stands and Technology (NIST) standard. The initial concentration of NO was diluted to about 400 ppb by the air stream supplied by a zero air generator (Thermo Environmental Inc., model 111). The desired humidity level of the NO flow was controlled at 70% (2100 ppmv) by passing the zero air streams through a humidification chamber. The gas streams were premixed completely by a gas blender and the flow rate was controlled at 4 L $min^{-1}$ by a mass flow controller. After the adsorption-desorption equilibrium among water vapor, gases and photocatalysts were achieved, and the lamp was turned on. The concentration of NO was continuously measured by a chemiluminescence NO analyzer (Thermo Environmental Instruments Inc., model 42c), which monitors NO, $NO_2$, and NO$x$ (NO$x$ represents NO + $NO_2$) with a sampling rate of 0.7 L $min^{-1}$. The reaction of NO with air was ignorable when performing a control experiment with or without light in the absence of photocatalyst.

## 3. Result and Discussion

Figure 1 shows the XRD patterns of the prepared samples. For all the samples exhibit five distinct peaks ($2\theta$ = 25.4, 38.1, 48.1, 53.9, and 55.6°) which represent the indices of (101), (004), (200), (105), and (211) planes of anatase $TiO_2$. The crystalline sizes of the samples prepared by adding 0, 1, 5, and 10 g urea estimated by Scherrer formula from the (101) peaks of anatase phase were 14, 13, 10, and 9 nm, respectively. This indicates that $TiO_2$ particles in the prepared samples are nanocrystalline in nature. The result also evidences the addition of urea could suppress undesirable sintering and agglomeration of $TiO_2$ particle during the thermal treatment. In this process, $TiO_2$ nanoparticle possibly formed via the following two consecutive reaction steps:

$$TiF_4 + 4H_2O \longleftrightarrow Ti(OH)_4 + 4HF \quad (1)$$

$$Ti(OH)_4 \longrightarrow TiO_2 + H_2O \quad (2)$$

In the absence of urea, the rate of hydrolysis and condensation reactions ((1) and (2)) is rather slow due to the high concentration of $H^+$. Consequently, fewer $TiO_2$ nanoclusters are formed which is beneficial to crystal growth, rather than aggregation and a product with large crystal size could be obtained. For the addition of urea in the reaction, the added urea is easily decomposed and the produced $NH_3 \cdot H_2O$ will react with HCl as shown in (3) and (4). Thus the acidity of reaction system is decreased which would favor the formation of more $TiO_2$ nanoclusters and results in smaller crystalline sizes of product [42, 43].

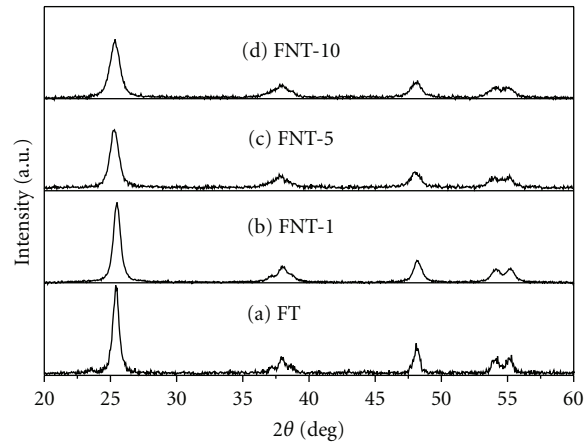


Figure 1: The X-ray diffraction patterns of fluorine-doped and fluorine- and nitrogen-codoped $TiO_2$ prepared at different conditions.

Consider the following:

$$CO(NH_2)_2 + 3H_2O \longrightarrow 2NH_3 \cdot H_2O + CO_2 \uparrow \quad (3)$$

$$2NH_3 \cdot H_2O + HCl \longrightarrow NH_4Cl + H_2O \quad (4)$$

Figure 2 depicts the SEM and TEM images of FNT-5. Figure 3(a) is the low-magnification image of the as-prepared FNT-5. It could be found that the as-prepared codoped sample consists entirely of small spherical particles with an average size of 200 nm~2 $\mu$m. Figure 3(b) is the magnified surface morphologies of typical codoped titania spheres showing the puckered surface of codoped titania, which will endow them with more active points and larger light-harvesting ability. The size and morphology of FNT-5 were further analyzed by TEM and HRTEM images. The TEM image confirms the puckered surface of the codoped sphere. Figure 3(d) is HRTEM images of the codoped $TiO_2$ sphere edge. Well-resolved lattice fringes are clearly visible, with an interplanar distance of 0.35 nm corresponding to the (101) d spacing of the anatase phase, further confirming the good crystallinity of as-prepared products.

Figure 3 shows the SEM images of the products fabricated under different conditions. Interestingly, it could be found that the presence of urea is determining the surface morphology of the product. In the case of the sample prepared without urea, it consists of spherical particles with a relative smooth surface morphology, while the solid spheres with puckered surface were obtained with the addition of urea and the quantity of added urea had not much effect on the morphology of final products.

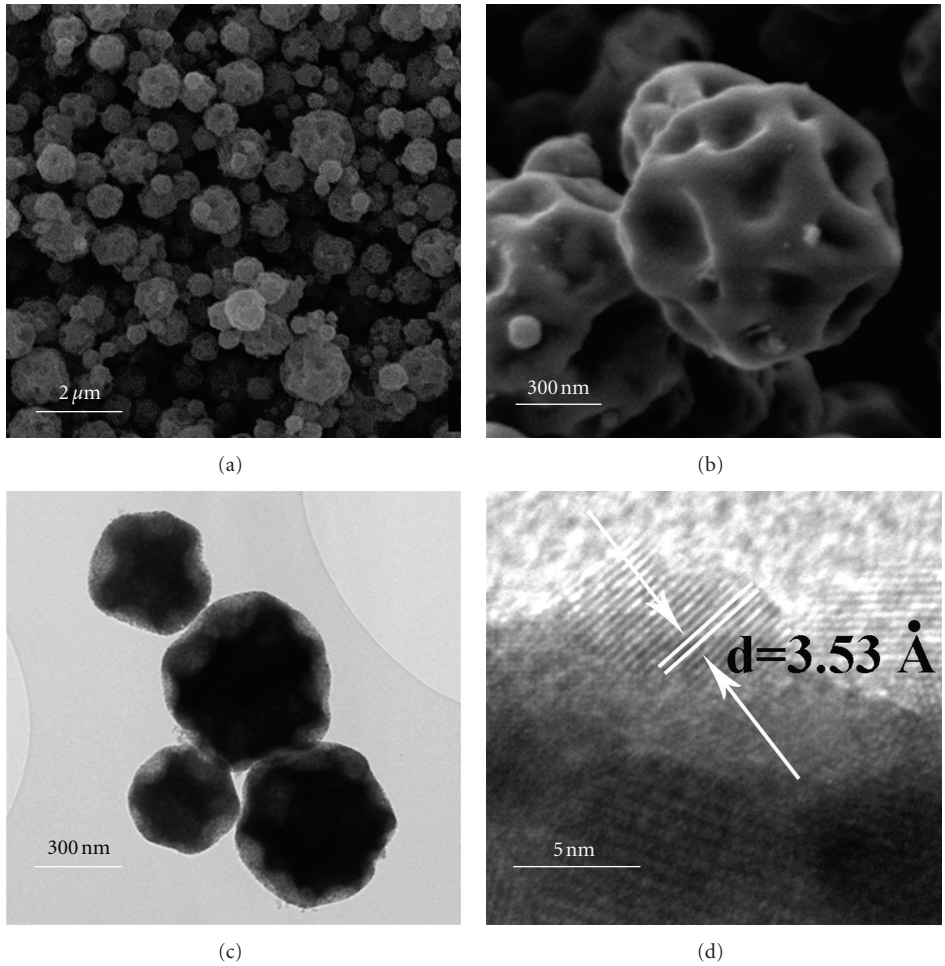


Figure 2: The morphology and structural characterization of FNT-5: (a) SEM image; (b) magnified SEM image; (c) TEM image; (d) HRTEM image.

On the basis of the above discussion, we propose the possible mechanisms for the special morphology of codoped product by the ultrasonic spray pyrolysis method. It is widely accepted that the droplets produced form nebulizer serve as microreactors and yield one particle per droplet when sprayed into a tubular reactor under pyrolysis condition. The size of droplet determines the product dimension [44]. The solvent was evaporated out of the droplets in the hot zone of the furnace, leading to the formation of microspheres. In this process, the hydrolysis velocity of Ti source plays a vital effect on the structure. For the samples without urea, the hydrolysis of $TiF_4$ was restrained due to the low pH value of reaction system, so the hydrolysis of $TiF_4$ happened after the volatilization of HCl in the aerosol (see Scheme 1(a)). Thus a product with hollow structure was obtained (see Figure S1(a) in Supplementary Material available online at doi:10.1155/2012/753429). While for the codoped samples, the formation process may follow the route shown in Scheme 1(b). The urea will react with HCl in the precursor solution, thus the $TiF_4$ was unstable and easily hydrolysis before the volatilization of liquid in the aerosol, hence getting the solid sphere (see Figure S1(b)). In addition, the surfaces of the products prepared under different condition have distinct difference. For the fluorine and nitrogen codoped samples, the urea in the precursor was decomposed easily and formed $NH_4Cl$ according to reaction of (3) and (4). Hence, there were some $NH_4Cl$ left in the sphere. The $NH_4Cl$ will be decomposed (5) at high temperature and cause the shrink of forming sphere with puckered surface. The $NH_3$ from the decomposed $NH_4Cl$ and the HF from the hydrolysis of $TiF_4$ would react with $TiO_2$ under high temperature (6), and consequently the codoped catalyst is obtained as follows:

$$NH_4Cl \longrightarrow NH_3 + HCl \tag{5}$$

$$Ti(OH)_4 + NH_3 + HF \longrightarrow TiO_{2-x-y}F_xN_y \tag{6}$$

The UV/Vis spectra of the prepared samples were recorded through the diffuse reflectance technique with the pure TiO2 (P25 Degussa) for comparison. The result is shown in Figure 4. Comparing with P25, the doped TiO2 spheres reveal a new absorption shoulder at 400–600 nm in the UV/Vis spectrum. The single doping of fluorine only has limited influence to light absorption properties of titania

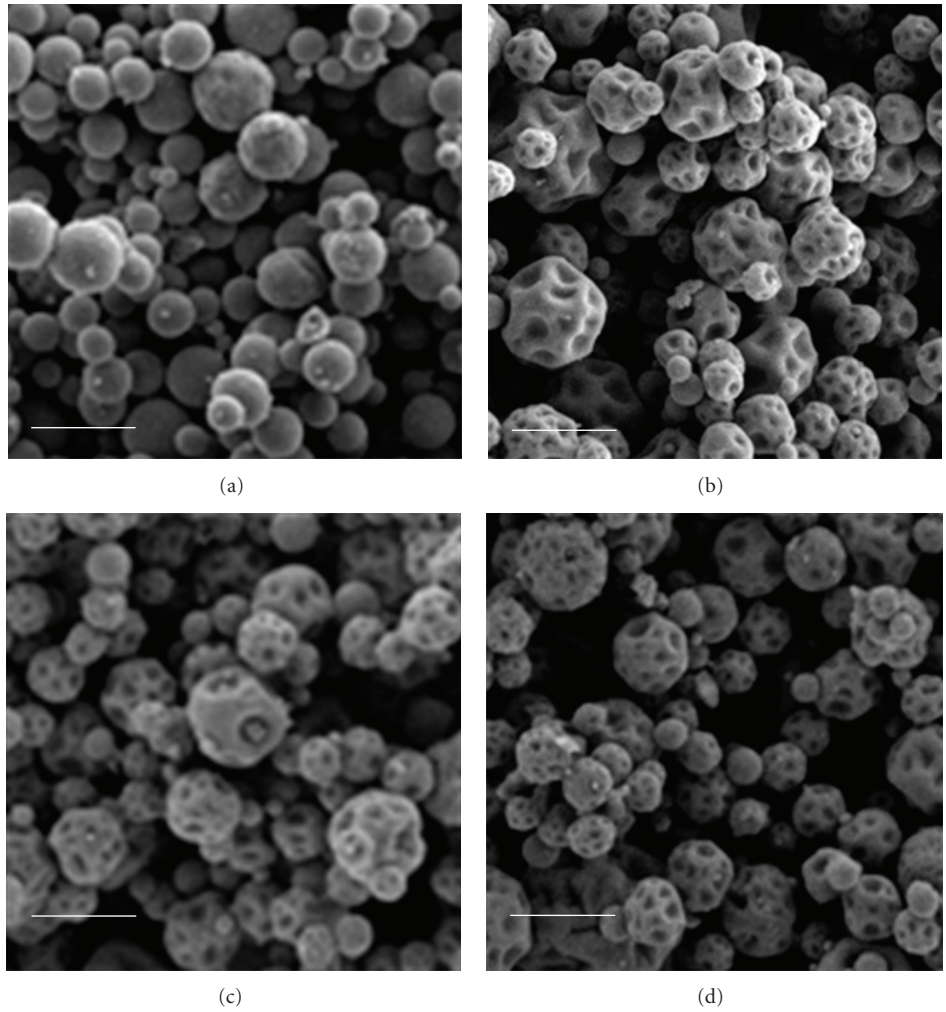


Figure 3: SEM images of fluorine- and nitrogen-codoped $TiO_2$ with different amount urea in the precursor solution: (a) FT; (b) FNT-1; (c) FNT-5; (d) FNT-10. The scale bar in the figure is 1 $\mu$m.

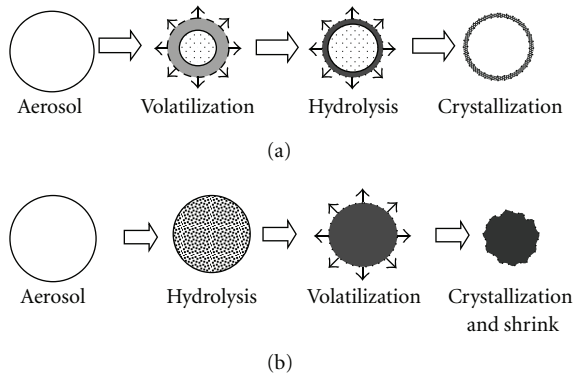


Scheme 1: Schematically illustrating the structure formation of FT and FNT via the ultrasonic spray pyrolysis process.

which only have a small shoulder at 400–450 nm. The F-doped-$TiO_2$ hollow spheres exhibit a slight tinge of light yellow color which could be due to the surface oxygen vacancies generated by the doping of fluorine [45, 46]. In comparison, the codoped samples have vivid yellow color and show a remarkable shift to visible-light region. Two optical absorption thresholds at about 535 and 440 nm in the visible range were observed for all the codoped $TiO_2$. These two absorption thresholds also demonstrate that two possible compositions have been introduced to $TiO_2$. The absorption threshold at about 440 nm is ascribed to the introduction of nitrogen to the $TiO_2$ lattice. The absorption edge of this band shifts towards higher wavelength on the whole with the increasing of urea quantity in precursor for all the codoped titania photocatalysts. The difference of the shift is due to the different amount of nitrogen doped into the $TiO_2$ framework as shown in the following XPS results. The absorption thresholds at about 535 nm are the superposition result of the nitrogen and fluorine doped into $TiO_2$ lattice. This enlarged light absorption range for the codoped samples in visible region will have great influence on their photocatalytic property.

The assessment of the surface chemical composition and electronic state of the product was investigated by using XPS analysis. The surface concentrations of fluorine and nitrogen

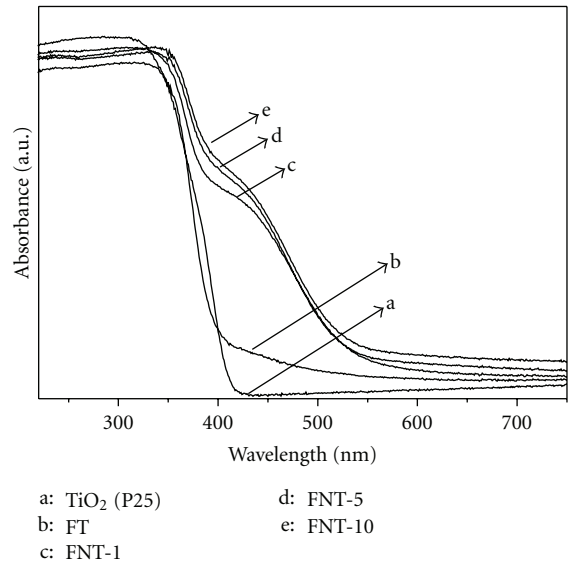


Figure 4: UV/Vis diffuse reflectance spectra of fluorine- and nitrogen-codoped $TiO_2$ with different urea in the precursor solution with pure $TiO_2$ (P25) for comparison.

Table 1: The quantitative XPS analysis result using the appropriate molar weight-correction factors.

| Sample name | F-atomic concentration | N-atomic concentration |
|---|---|---|
| FT | 4.0% | — |
| FNT-1 | 1.46% | 1.38% |
| FNT-5 | 1.62% | 2.38% |
| FNT-10 | 1.81% | 3.65% |

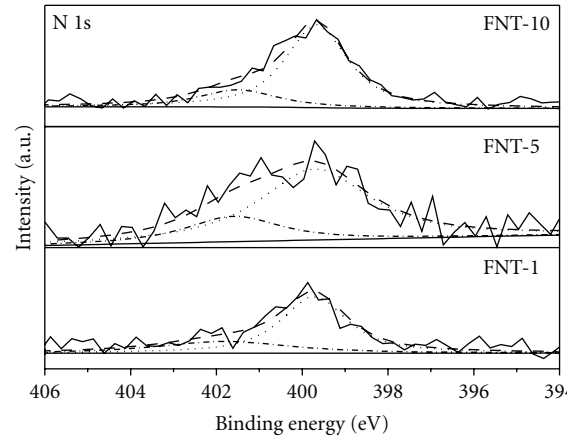


Figure 5: The N 1s spectra of fluorine and nitrogen codoped $TiO_2$ with different urea in the precursor solution.

in these photocatalysts are summarized in Table 1. It could be found that the fluorine and nitrogen concentration increased with increasing urea in the precursor. It was obvious that the increased N dopant is due to more nitrogen resource from urea. While for the fluorine, the HF in the codoping system may react with the $NH_3$ which was produced by the urea decomposition and get $NH_4F$. The boiling point of $NH_4F$ (64.6°C) is much higher than that of HF (19.4°C) which could reduce the fluorine specie losing by the evaporation in the reaction. Thus more fluorine will be doped into $TiO_2$ with the increased amount of urea. The high-resolution XPS spectra of N 1s and F 1s are shown in Figures 5 and 6. The N 1s regions of all samples are asymmetric, indicating that there are at least two kinds of chemical states. Using XPSPEAK software, N 1s region could be fitted to two peaks. The binding energy region near 399.5 eV is derived from the presence of O–Ti–N linkages in the crystalline $TiO_2$ lattice [47]. It has been proved that this nitrogen state is responsible for the observed shift of the photochemical threshold of $TiO_2$ [48, 49], while the N 1s peaks at 401.6 eV are arisen from the N atoms from adventitious N–N, N–O, or NHX adsorbed on the surface of the sample [50–52]. Figure 6 gives the F 1s XPS spectra and a wide and symmetrical peaks at 685 eV were observed which could be assigned to the substitutional fluorine in titania lattice [53].

The oxidation of NO under the irradiation of visible light was used to evaluate the photocatalytic activity of the samples prepared under different condition. It is found that NO could be oxidized over the catalysts prepared under different conditions when the visible light was switched on. The control experiment found that the photolysis of NO without photocatalysts or use pure $TiO_2$ (P25) was negligible under the same condition. Consequently, it could be concluded that all the samples have visible-light-driven photocatalytic activity. Table 2 shows the photocatalytic activity of codoped $TiO_2$ for NO oxidation irradiated by visible light with the fluorine single-doped sample for comparison. As expected, the codping greatly affects the photocatalytic activity of spherical $TiO_2$ toward oxidizing NO in gasphase. For the single fluorine doping sample, the NO photocatalytic oxidation rate is 190.7 $\mu$mol/mol·h. The oxygen vacancy created by the doped fluorine slightly extended the optical absorption of $TiO_2$ in the visible-light region to contribute to the visible-light photocatalytic activity of fluorine doping sample [54]. However, the activity of single doping of fluorine is limited as the doping of fluorine could not alter the basic band structure of $TiO_2$. For the codoped samples, they show high oxidation rate under optimal conditions. For the sample of FNT-10, the NO photocatalytic oxidation rate is 287.4 $\mu$mol/mol·h which is about 50% higher than that of FT. The enhanced activity of FNT-10 can be ascribed to the following two reasons. Firstly, the improved visible-light absorption and red shift of codoped $TiO_2$ which would lead to increased number of photons that take part in the photocatalytic reaction. Second, the small crystal size of codoped $TiO_2$ is a benefit to its photocatalytic performance. With a smaller particle size, the number of active surface sites increases, and so does the surface charge carrier transfer rate in photocatalysis. Therefore the higher photocatalytic performance is obtained [55].

The results also show that the activities of codoped samples were greatly influenced by the quantity of added urea in the precursor solution. The photocatalytic activity

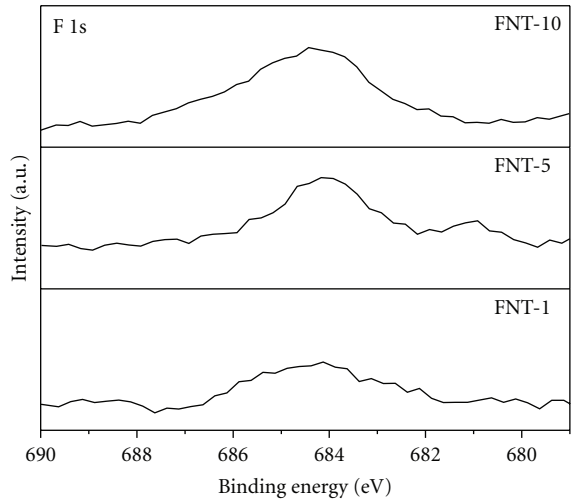


Figure 6: The F 1s spectra of fluorine- and nitrogen-codoped $TiO_2$ with different urea in the precursor solution.

Table 2: The photocatalytic oxidation rate of NO under the irradiation of visible light over the catalyst prepared under different conditions.

| Sample name | FT | FNT-1 | FNT-5 | FNT-10 |
|---|---|---|---|---|
| Oxidation rate[a] | 190.7 | 142.1 | 198.1 | 287.4 |

[a] Oxidation rate: $n$ (nitric oxide) per mol of catalyst per hour ($\mu$mol/mol·h).

of samples decreased with the decreasing amount of added urea. This is due to more fluorine and nitrogen atoms that were doped into $TiO_2$ lattice and the smaller crystalline sizes for the samples prepared with more urea in the precursor. While if we further increased the amount of urea (>10 g) in the preparation, the precursor solution was not stable and some sedimentation was formed, thus we could not get the codoped $TiO_2$ with ultrasonic spray pyrolysis method.

## 4. Conclusion

In summary, the fluorine- and nitrogen-codoped $TiO_2$ spheres with puckered surface have been fabricated via an ultrasonic spray pyrolysis method. Increasing the addition of urea from 1 g to 10 g makes more nitrogen and fluorine doped into $TiO_2$ lattice and resulted in a new strong absorption band in the visible range. Activity test shows that the fluorine and nitrogen codoped $TiO_2$ could efficiently photocatalytically oxidize NO under visible-light irradiation and the activity was higher than that of fluorine-doped $TiO_2$. This facile method may be easily scaled up for industrial production. Similar doping or codoping with other nonmetal and metal ions (S, Cl, Br, B, Pt, and Fe) with this method should lead to the development of new kind of spherical semiconductor composites, which are promising candidates as multifunctional materials as catalysts, photocatalysts, and optoelectronic materials.

## Acknowledgments

This work was supported by the Research Grants Council of Hong Kong, the internal funding of Hong Kong Institute of Education and National Natural Science Foundation of China (21103095), the Natural Science Foundation of Fujian province (2010J05030), and the Excellent Young Scientific Research Talents in University of Fujian, China (JA12285).

## References

[1] J. Heinrich, "Influence of indoor factors in dwellings on the development of childhood asthma," *International Journal of Hygiene and Environmental Health*, vol. 214, no. 1, pp. 1–25, 2011.

[2] C. Nguyen, C. G. Sonwane, S. K. Bhatia, and D. D. Do, "Adsorption of benzene and ethanol on MCM-41 material," *Langmuir*, vol. 14, no. 17, pp. 4950–4952, 1998.

[3] E. N. Coker, C. Jia, and H. G. Karge, "Adsorption of benzene and benzene derivatives onto zeolite H-Y studied by microcalorimetry," *Langmuir*, vol. 16, no. 3, pp. 1205–1210, 2000.

[4] K. Yu and G. W. M. Lee, "Decomposition of gas-phase toluene by the combination of ozone and photocatalytic oxidation process ($TiO_2$/UV, $TiO_2$/UV/$O_3$, and UV/$O_3$)," *Applied Catalysis B*, vol. 75, no. 1-2, pp. 29–38, 2007.

[5] M. Koch, D. R. Cohn, R. M. Patrick et al., "Electron beam atmospheric pressure cold plasma decomposition of carbon tetrachloride and trichloroethylene," *Environmental Science and Technology*, vol. 29, no. 12, pp. 2946–2952, 1995.

[6] J. C. Yu, J. G. Yu, L. Z. Zhang, and W. K. Ho, "Enhancing effects of water content and ultrasonic irradiation on the photocatalytic activity of nano-sized $TiO_2$ powders," *Journal of Photochemistry and Photobiology A*, vol. 148, no. 1–3, pp. 263–271, 2002.

[7] H. F. Xu, G. Vanamu, H. Konishi, R. Yeredla, J. Phillips, and Y. F. Wang, "Photocatalytic oxidation of a volatile organic component of acetaldehyde using titanium oxide nanotubes," *Journal of Nanomaterials*, vol. 2006, Article ID 78902, 8 pages, 2006.

[8] J. G. Yu, H. G. Yu, B. Cheng, X. J. Zhao, and Q. J. Zhang, "Preparation and photocatalytic activity of mesoporous anatase $TiO_2$ nanofibers by a hydrothermal method," *Journal of Photochemistry and Photobiology A*, vol. 182, no. 2, pp. 121–127, 2006.

[9] X. F. Chen, X. C. Wang, and X. Z. Fu, "Hierarchical macro/mesoporous $TiO_2$/$SiO_2$ and $TiO_2$/$ZrO_2$ nanocomposites for environmental photocatalysis," *Energy & Environmental Science*, vol. 2, no. 8, pp. 872–877, 2009.

[10] K. Wilke and H. D. Breuer, "The influence of transition metal doping on the physical and photocatalytic properties of titania," *Journal of Photochemistry and Photobiology A*, vol. 121, no. 1, pp. 49–53, 1999.

[11] J. S. Zhang, X. F. Chen, K. Takanabe et al., "Synthesis of a carbon nitride structure for visible-light catalysis by copolymerization," *Angewandte Chemie*, vol. 49, no. 2, pp. 441–444, 2010.

[12] H. Irie, S. Washizuka, N. Yoshino, and K. Hashimoto, "Visible-light induced hydrophilicity on nitrogen-substituted titanium dioxide films," *Chemical Communications*, vol. 9, no. 11, pp. 1298–1299, 2003.

[13] S. Horikoshi, Y. Minatodani, H. Sakai, M. Abe, and N. Serpone, "Characteristics of microwaves on second generation

nitrogen-doped $TiO_2$ nanoparticles and their effect on photoassisted processes," *Journal of Photochemistry and Photobiology A*, vol. 217, no. 1, pp. 191–200, 2011.

[14] W. Guo, L. Q. Wu, Z. Chen, G. Boschloo, A. Hagfeldt, and T. L. Ma, "Highly efficient dye-sensitized solar cells based on nitrogen-doped titania with excellent stability," *Journal of Photochemistry and Photobiology A*, vol. 219, no. 2-3, pp. 180–187, 2011.

[15] J. G. Yu, J. C. Yu, B. Cheng, S. K. Hark, and K. Iu, "The effect of $F^-$ doping and temperature on the structural and textural evolution of mesoporous $TiO_2$ powders," *Journal of Solid State Chemistry*, vol. 174, no. 2, pp. 372–380, 2003.

[16] J. S. Jang, H. G. Kim, S. M. Ji et al., "Formation of crystalline $TiO_2$-xNx and its photocatalytic activity," *Journal of Solid State Chemistry*, vol. 179, no. 4, pp. 1067–1075, 2006.

[17] Y. Xie, X. Zhao, Y. Chen, Q. Zhao, and Q. Yuan, "Preparation and characterization of porous C-modified anatase titania films with visible light catalytic activity," *Journal of Solid State Chemistry*, vol. 180, no. 12, pp. 3576–3582, 2007.

[18] J. C. Yu, W. K. Ho, J. G. Yu, H. Y. Yip, P. K. Wong, and J. C. Zhao, "Efficient visible-light-induced photocatalytic disinfection on sulfur-doped nanocrystalline titania," *Environmental Science & Technology*, vol. 39, no. 4, pp. 1175–1179, 2005.

[19] R. Asahi, T. Morikawa, T. Ohwaki, K. Aoki, and Y. Taga, "Visible-light photocatalysis in nitrogen-doped titanium oxides," *Science*, vol. 293, no. 5528, pp. 269–271, 2001.

[20] H. Irie, Y. Watanabe, and K. Hashimoto, "Nitrogen-concentration dependence on photocatalytic activity of $TiO_2$-xNx powders," *Journal of Physical Chemistry B*, vol. 107, no. 23, pp. 5483–5486, 2003.

[21] Q. C. Xu, D. V. Wellia, S. Yan, D. W. Liao, T. M. Lim, and T. T. Y. Tan, "Enhanced photocatalytic activity of C-N-codoped $TiO_2$ films prepared via an organic-free approach," *Journal of Hazardous Materials*, vol. 188, no. 1V3, pp. 172–180, 2011.

[22] J. A. Rengifo-Herrera, K. Pierzchała, A. Sienkiewicz et al., "Synthesis, characterization, and photocatalytic activities of nanoparticulate N, S-codoped $TiO_2$ having different surface-to-volume ratios," *Journal of Physical Chemistry C*, vol. 114, no. 6, pp. 2717–2723, 2010.

[23] H. J. Tian, L. H. Hu, W. X. Li, J. Sheng, S. Xu, and S. Dai, "A facile synthesis of anatase N,B codoped $TiO_2$ anodes for improved-performance dye-sensitized solar cells," *Journal of Materials Chemistry*, vol. 21, no. 20, pp. 7074–7077, 2011.

[24] R. Long and N. J. English, "First-principles calculation of synergistic (N, P)-codoping effects on the visible-light photocatalytic activity of anatase $TiO_2$," *Journal of Physical Chemistry C*, vol. 114, no. 27, pp. 11984–11990, 2010.

[25] W. Ho, J. C. Yu, and S. C. Lee, "Synthesis of hierarchical nanoporous F-doped $TiO_2$ spheres with visible light photocatalytic activity," *Chemical Communications*, no. 10, pp. 1115–1117, 2006.

[26] Y. L. Su, X. W. Zhang, M. H. Zhou, S. Han, and L. C. Lei, "Preparation of high efficient photoelectrode of N-F-codoped $TiO_2$ nanotubes," *Journal of Photochemistry and Photobiology A*, vol. 194, no. 2-3, pp. 152–160, 2008.

[27] D. Li, N. Ohashi, S. Hishita, T. Kolodiazhnyi, and H. Haneda, "Origin of visible-light-driven photocatalysis: a comparative study on N/F-doped and N-F-codoped $TiO_2$ powders by means of experimental characterizations and theoretical calculations," *Journal of Solid State Chemistry*, vol. 178, no. 11, pp. 3293–3302, 2005.

[28] S. Livraghi, K. Elghniji, A. M. Czoska, M. C. Paganini, E. Giamello, and M. Ksibi, "Nitrogen-doped and nitrogen-fluorine-codoped titanium dioxide. Nature and concentration of the photoactive species and their role in determining the photocatalytic activity under visible light," *Journal of Photochemistry and Photobiology A*, vol. 205, no. 2-3, pp. 93–97, 2009.

[29] D. G. Huang, S. J. Liao, J. M. Liu, Z. Dang, and L. Petrik, "Preparation of visible-light responsive N-F-codoped $TiO_2$ photocatalyst by a sol-gel-solvothermal method," *Journal of Photochemistry and Photobiology A*, vol. 184, no. 3, pp. 282–288, 2006.

[30] J. Xu, B. Yang, M. Wu, Z. Fu, Y. Lv, and Y. Zhao, "Novel N-F-codoped $TiO_2$ inverse opal with a hierarchical meso-/macroporous structure: synthesis, characterization, and photocatalysis," *Journal of Physical Chemistry C*, vol. 114, no. 36, pp. 15251–15259, 2010.

[31] S. W. Hu, J. Zhu, L. Wu et al., "Effect of fluorination on photocatalytic degradation of rhodamine B over in(OH)ySz: promotion or Suppression?" *The Journal of Physical Chemistry C*, vol. 115, no. 2, pp. 460–467, 2011.

[32] J. C. Yu, J. G. Yu, W. K. Ho, Z. T. Jiang, and L. Z. Zhang, "Effects of F-doping on the photocatalytic activity and microstructures of nanocrystalline $TiO_2$ powders," *Chemistry of Materials*, vol. 14, no. 9, pp. 3808–3816, 2002.

[33] A. Vijayabalan, K. Selvam, R. Velmurugan, and M. Swaminathan, "Photocatalytic activity of surface fluorinated $TiO_2$-P25 in the degradation of Reactive Orange 4," *Journal of Hazardous Materials*, vol. 172, no. 2-3, pp. 914–921, 2009.

[34] Q. Wang, C. Chen, W. Ma, H. Zhu, and J. Zhao, "Pivotal role of fluorine in tuning band structure and visible-light photocatalytic activity of nitrogen-doped $TiO_2$," *Chemistry*, vol. 15, no. 19, pp. 4765–4769, 2009.

[35] G. W. Koebrugge, L. Winnubst, and A. J. Burggraaf, "Thermal stability of nanostructured titania and titania-ceria ceramic powders prepared by the sol-gel process," *Journal of Materials Chemistry*, vol. 3, no. 11, pp. 1095–1100, 1993.

[36] S. J. Kim, S. D. Park, Y. H. Jeong, and S. Park, "Homogeneous precipitation of $TiO_2$ ultrafine powders from aqueous $TiOCl_2$ solution," *Journal of the American Ceramic Society*, vol. 82, no. 4, pp. 927–932, 1999.

[37] H. B. Yin, Y. Wada, T. Kitamura et al., "Hydrothermal synthesis of nanosized anatase and ruffle $TiO_2$ using amorphous phase $TiO_2$," *Journal of Materials Chemistry*, vol. 11, no. 6, pp. 1694–1703, 2001.

[38] S. E. Skrabalak and K. S. Suslick, "Carbon powders prepared by ultrasonic spray pyrolysis of substituted alkali benzoates," *Journal of Physical Chemistry C*, vol. 111, no. 48, pp. 17807–17811, 2007.

[39] K. D. Kim, K. Y. Choi, and J. W. Yang, "Formation of spherical hollow silica particles from sodium silicate solution by ultrasonic spray pyrolysis method," *Colloids and Surfaces A*, vol. 254, no. 1–3, pp. 193–198, 2005.

[40] Z. Ai, L. Zhang, and S. Lee, "Efficient visible light photocatalytic oxidation of NO on aerosol flow-synthesized nanocrystalline $InVO_4$ hollow microspheres," *Journal of Physical Chemistry C*, vol. 114, no. 43, pp. 18594–18600, 2010.

[41] Y. Huang, Z. Ai, W. Ho, M. Chen, and S. Lee, "Ultrasonic spray pyrolysis synthesis of porous Bi2WO6 microspheres and their visible-light-induced photocatalytic removal of NO," *The Journal of Physical Chemistry A*, vol. 114, no. 14, pp. 6342–6349, 2010.

[42] X. Z. Li and F. B. Li, "Study of $Au/Au^{3+}$-$TiO_2$ photocatalysts toward visible photooxidation for water and wastewater treatment," *Environmental Science & Technology*, vol. 35, no. 11, pp. 2381–2387, 2001.

[43] M. Zhou, J. Yu, and H. Yu, "Effects of urea on the microstructure and photocatalytic activity of bimodal mesoporous titania microspheres," *Journal of Molecular Catalysis A*, vol. 313, no. 1-2, pp. 107–113, 2009.

[44] J. Zhang, A. Elsanousi, J. Lin et al., "Aerosol-assisted self-assembly of aluminum borate ($Al_{18}B_4O_{33}$) nanowires into three dimensional hollow spherical architectures," *Crystal Growth and Design*, vol. 7, no. 12, pp. 2764–2767, 2007.

[45] A. G. Kontos, M. Pelaez, V. Likodimos, N. Vaenas, D. D. Dionysiou, and P. Falaras, "Visible light induced wetting of nanostructured N-F co-doped titania films," *Photochemical & Photobiological Sciences*, vol. 10, no. 3, pp. 350–354, 2011.

[46] I. N. Martyanov, S. Uma, S. Rodrigues, and K. J. Klabunde, "Structural defects cause $TiO_2$-based photocatalysts to be active in visible light," *Chemical Communications*, vol. 10, no. 21, pp. 2476–2477, 2004.

[47] T. L. Ma, M. Akiyama, E. Abe, and I. Imai, "High-efficiency dye-sensitized solar cell based on a nitrogen-doped nanostructured titania electrode," *Nano Letters*, vol. 5, no. 12, pp. 2543–2547, 2005.

[48] O. Diwald, T. L. Thompson, T. Zubkov, E. G. Goralski, S. D. Walck, and J. T. Yates, "Photochemical activity of nitrogen-doped rutile $TiO_2(110)$ in visible light," *Journal of Physical Chemistry B*, vol. 108, no. 19, pp. 6004–6008, 2004.

[49] J. Fang, F. Shi, J. Bu et al., "One-step synthesis of bifunctional $TiO_2$ catalysts and their photocatalytic activity," *Journal of Physical Chemistry C*, vol. 114, no. 17, pp. 7940–7948, 2010.

[50] J. L. Gole, J. D. Stout, C. Burda, Y. Lou, and X. Chen, "Highly efficient formation of visible light tunable $TiO_2$-xNx photocatalysts and their transformation at the nanoscale," *Journal of Physical Chemistry B*, vol. 108, no. 4, pp. 1230–1240, 2004.

[51] S. Sakthivel and H. Kisch, "Photocatalytic and photoelectrochemical properties of nitrogen-doped titanium dioxide," *ChemPhysChem*, vol. 4, no. 5, pp. 487–490, 2003.

[52] J. A. Rodriguez, T. Jirsak, G. Liu, J. Hrbek, J. Dvorak, and A. Maiti, "Chemistry of $NO_2$ on oxide surfaces: formation of $NO_3$ on $TiO_2(110)$ and $NO_2 \leftrightarrow O$ vacancy interactions," *Journal of the American Chemical Society*, vol. 123, no. 39, pp. 9597–9605, 2001.

[53] D. Li, H. Haneda, S. Hishita, and N. Ohashi, "Visible-light-driven nitrogen-doped $TiO_2$ photocatalysts: effect of nitrogen precursors on their photocatalysis for decomposition of gas-phase organic pollutants," *Materials Science and Engineering B*, vol. 117, no. 1, pp. 67–75, 2005.

[54] D. Li, H. Haneda, S. Hishita, and N. Ohashi, "Visible-light-driven N-F-codoped $TiO_2$ photocatalysts. 2. Optical characterization, photocatalysis, and potential application to air purification," *Chemistry of Materials*, vol. 17, no. 10, pp. 2596–2602, 2005.

[55] J. Zhu, J. Yang, Z. F. Bian et al., "Nanocrystalline anatase $TiO_2$ photocatalysts prepared via a facile low temperature nonhydrolytic sol-gel reaction of $TiCl_4$ and benzyl alcohol," *Applied Catalysis B*, vol. 76, no. 1-2, pp. 82–91, 2007.